Combined *in situ* solid-state NMR, UV/Vis, and on-line GC studies of heterogeneously catalyzed reactions under continuous flow conditions

Spectroscopic background: The *in situ* flow MAS NMR technique (see Topic "3" of link "*In Situ* Solid-State NMR Techniques") allows investigations of **the steady state of heterogeneously catalyzed reactions**, which is particularly interesting if **catalytically active deposits** contribute to the mechanism of these reactions. One of the heterogeneously catalyzed reactions being in the focus of research is the **methanol-to-olefin (MTO)** and, more recently, the **methanol-to-propene (MTP)** conversion on Broensted acidic catalysts. Methanol is primarily derived from natural gas, where steam reforming converts the various light hydrocarbons in natural gas (primarily methane) into carbon monoxide and hydrogen. Subsequently, methanol is produced by hydrogenation of carbon monoxide. Via the MTO and MTP conversion on zeolites, a broad variety of olefins can be obtained, depending on the structure type and acid sites of the catalyst as well as the reaction conditions [1-13].

Scheme 1 shows a concept for the conversion of methanol-to-hydrocarbons over zeolite H-ZSM-5, which is named **dual-cycle mechanism** [3]. While for zeolite H-ZSM-5 with a crossing 10-ring pore system the olefin-based cycle (left) dominates, the aromatic-based cycle (right) plays an important role for zeolite catalysts with small oxygen windows and small cages, such as SAPO-34 (diameter of 8-ring windows of ca. 3.8 Å, cage diameter of ca. 9.4 Å) [2].

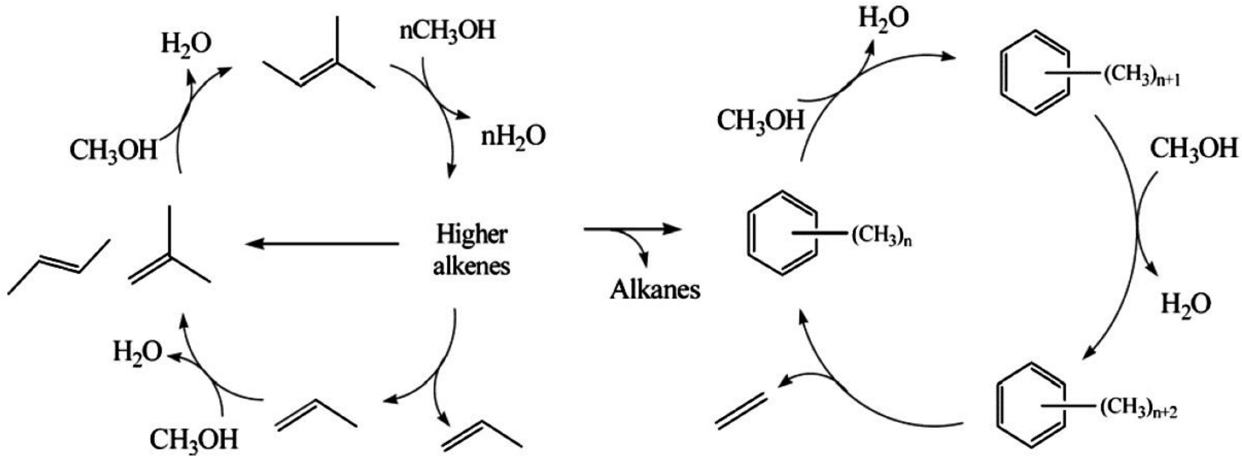

Scheme 1

The large **olefins and alkylated aromatics** contributing to the dual-cycle mechanism have a **long residence time on the catalysts** and are, therefore, available for ***in situ*** **continuous flow MAS NMR spectroscopy combined with on-line GC analysis** of the volatile reaction products [14-19]. Furthermore, UV/Vis spectroscopy is sensitive for numerous of these hydrocarbon-pool compounds, such as dienes, aromatics, and carbenium ions (see **Table 1**) [18]. Therefore, the above-mentioned *in situ* technique was **additionally combined with *in situ* UV/Vis spectroscopy** (see Sections "flow probe 2" and "flow probe 3" via link "*In Situ* Solid-State NMR Techniques") for studies of the methanol conversion on Broensted acidic zeolite catalysts [16, 18, 19].

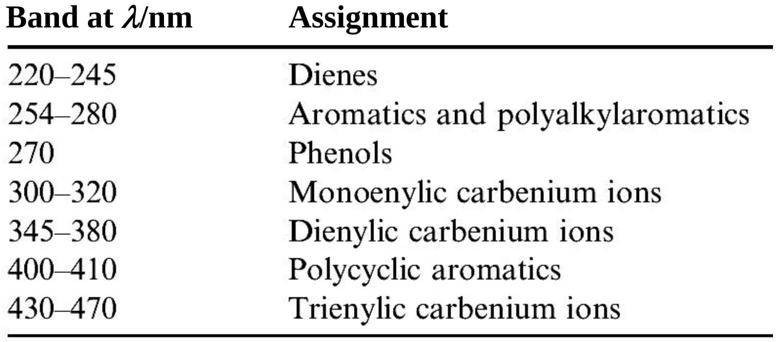

Band at λ/nm	Assignment
220–245	Dienes
254–280	Aromatics and polyalkylaromatics
270	Phenols
300–320	Monoenylic carbenium ions
345–380	Dienylic carbenium ions
400–410	Polycyclic aromatics
430–470	Trienylic carbenium ions

Table 1

Fig. 1 shows *in situ* ^{13}C MAS NMR and UV/Vis spectra recorded during the conversion of ^{13}C-enriched methanol on the silicoaluminophosphate H-SAPO-34 under continuous-flow conditions at reaction temperatures of T = 473 (a) to 673 K (d) [18]. The yields of volatile reaction products, such as dimethyl ether (DME), ethene ($C_{2=}$), propene ($C_{3=}$), and butenes ($C_{4=}$), were simultaneously analyzed by on-line GC and are given on the left-hand side of **Fig. 1**.

At temperatures of T = 473 K and 523 K (**Figs. 1a and 1b**), the conversion of methanol is dominated by the formation of DME. This is indicated by the on-line GC data and by the ^{13}C MAS NMR signals of adsorbed methanol at δ_{13C} = 50 ppm and DME at δ_{13C} = 61 ppm (see also **Table 2** [18]). The simultaneously recorded UV/Vis spectra of surface species formed during the methanol conversion are depicted on the right-hand side. Already at T = 473 K, UV/Vis sensitive species begin to be formed causing the band of dienes at λ = 245 nm (**Table 1**). The concentration of these dienes is too small for their detection by ^{13}C MAS NMR spectroscopy.

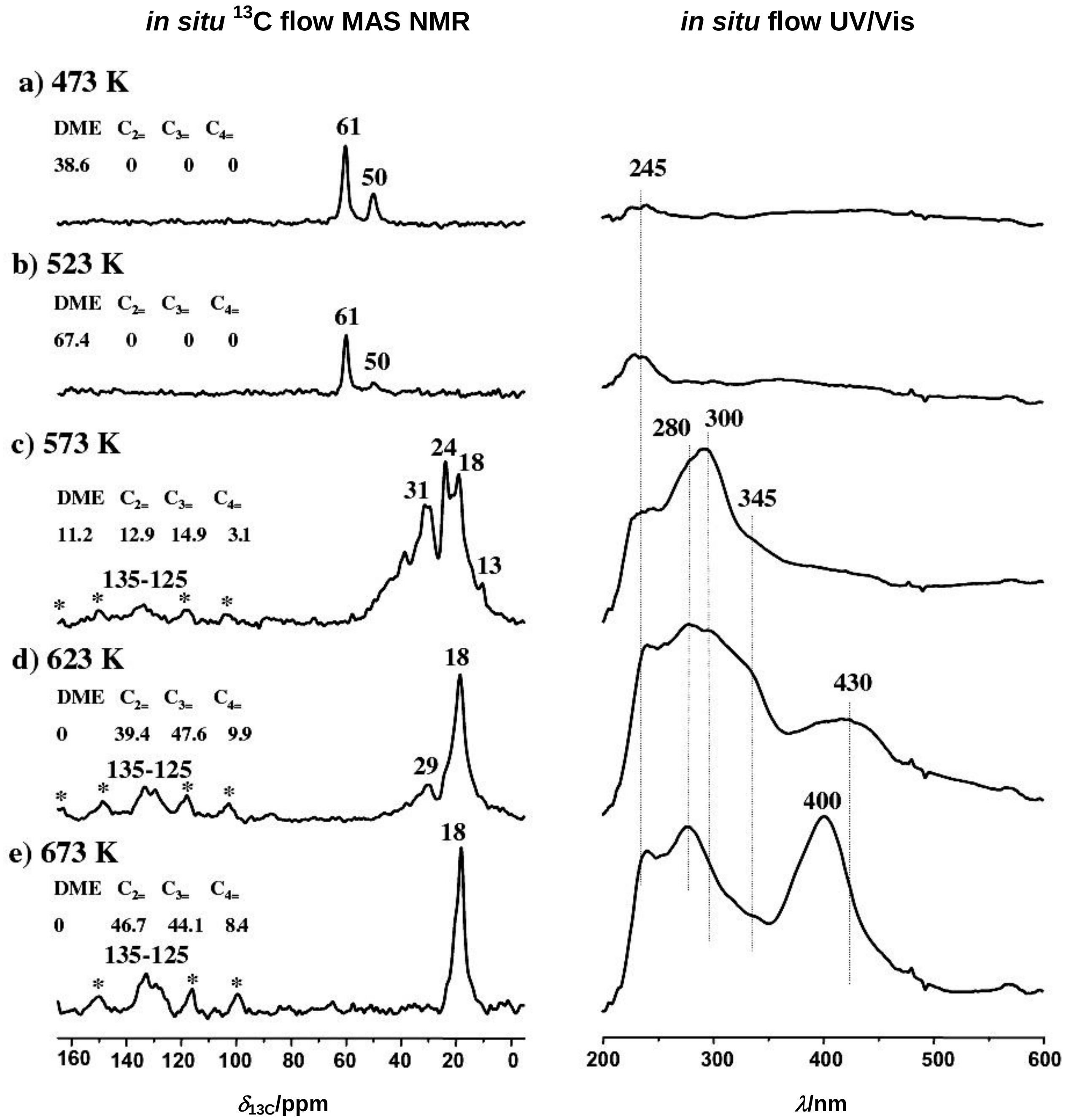

Fig. 1

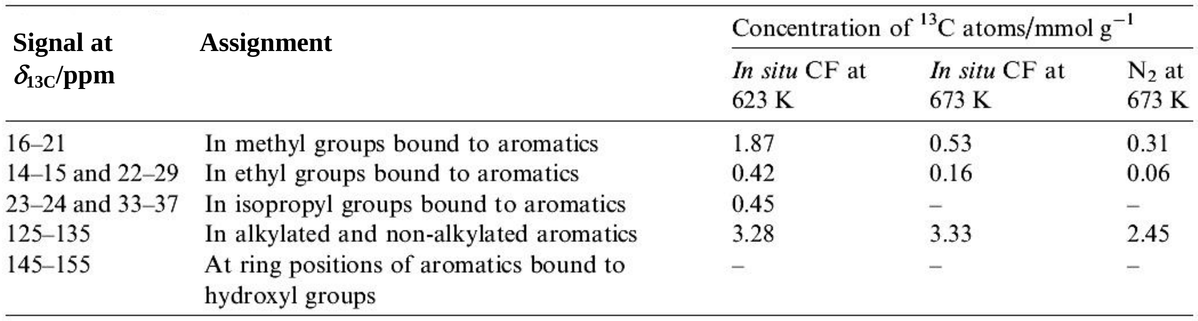

Signal at δ_{13C}/ppm	Assignment	Concentration of ^{13}C atoms/mmol g^{-1}		
		In situ CF at 623 K	*In situ* CF at 673 K	N_2 at 673 K
16–21	In methyl groups bound to aromatics	1.87	0.53	0.31
14–15 and 22–29	In ethyl groups bound to aromatics	0.42	0.16	0.06
23–24 and 33–37	In isopropyl groups bound to aromatics	0.45	–	–
125–135	In alkylated and non-alkylated aromatics	3.28	3.33	2.45
145–155	At ring positions of aromatics bound to hydroxyl groups	–	–	–

Table 2

At *T* = 573 K (**Fig.1c**), most of the methanol and DME molecules are converted. New ^{13}C MAS NMR signals appear at δ_{13C} = 10 to 40 ppm and δ_{13C} = 125 to 135 ppm, which indicate the formation of polyalkylaromatics. Simultaneously, a strong increase of the yields of light olefins was observed by on-line GC analysis. The UV/Vis spectrum recorded at *T* = 573 K consists of a dominating band at λ = 300 nm due to the formation of monoenylic carbenium ions (**Table 1**). Furthermore, additional bands appear as weak shoulders at λ = 280 nm and 345 nm, attributed to polyalkylaromatics and dienylic carbenium ions (**Table 1**). These findings indicate that olefinic compounds react with monoenylic carbenium ions to dienylic carbenium ions and aromatic compounds.

At *T* = 623 K (**Fig. 1d**), a further increase of the yields of light olefins, but no DME was found by on-line GC analysis. The low-shift range of the ^{13}C MAS NMR spectrum is dominated by a signal at δ_{13C} = 18 ppm due to methyl groups bound to aromatics, while most of the other signals in the region of alkyl groups occurring at lower reaction temperatures disappeared. Simultaneously, the intensities of the ^{13}C MAS NMR signals of aromatic compounds at δ_{13C} = 125 to 135 ppm increased. The UV/Vis spectrum recorded at *T* = 623 K is dominated by a band at λ = 280 nm with shoulders at λ = 300 and 345 nm due to polyalkylaromatics and monoenylic and dienylic carbenium ions, respectively. In addition, a broad band appeared at λ = 430 nm, which is generally explained by trienylic carbenium ions (**Table 1**).

The UV/Vis spectra recorded at *T* = 573 to 623 K hint at a reaction of olefins with reactive carbenium ions leading to higher carbenium ions with a maximum of three conjugated double bonds. Up to the formation of dienylic carbenium ions, this pathway may contribute to the formation of aromatic hydrocarbon-pool compounds. The presence of trienylic carbenium ions is an indication for the formation of larger organic deposits, such as carbenium ions formed by polycyclic aromatics. In agreement with the above-mentioned finding, the UV/Vis spectrum recorded at *T* = 673 K (**Fig. 1e**) shows a strong band at λ = 400 nm due to non-protonated polycyclic aromatics, such as polymethylanthracenes. The bands of carbenium ions at λ = 345 nm and 430 nm decreased, and at low wavelengths exclusively bands of dienes and polyalkylaromatics appear at λ = 245 nm and 280 nm, respectively. The simultaneously recorded ^{13}C MAS NMR spectrum consists of signals at δ_{13C} = 18 ppm and ca. 135 ppm (**Fig. 1e, left**), which are caused by polymethylaromatics

(**Table 2**). In agreement with the results of UV/Vis spectroscopy, the broad ^{13}C MAS NMR signal at δ_{13C} = 125 ppm indicates the formation of polycyclic aromatics.

In **Fig. 2a, left**, the ^{13}C MAS NMR spectrum of H-SAPO-34 recorded at room temperature after methanol-to-olefin conversion at T = 673 K for 3 h (used H-SAPO-34 catalyst) is shown. The concentration of organic deposits in the chabazite cages ($T_{12}O_{24}$: 1.38 mmol/g) of H-SAPO-34 was determined by simulation of the spectral range of the ^{13}C MAS NMR signals caused by ^{13}C atoms in alkyl groups and aromatic rings and the comparison of these intensities with an external intensity standard (dehydrated H-SAPO-34 loaded with $^{13}CH_3OH$).

In columns 3 and 4 of **Table 2**, the concentration of ^{13}C atoms contributing to alkyl groups and aromatic rings are given for the organic deposits formed on H-SAPO-34. Upon methanol conversion at T = 623 K, aromatic compounds with 3.28 mmol ^{13}C atoms or 0.55 mmol aromatic rings per gram were formed corresponding to ca. 0.4 benzene rings per chabazite cage. These aromatic compounds are alkylated by a mean number of 2.23 mmol methyl, ethyl, and propyl groups per gram corresponding to ca. 4.1 alkyl groups per aromatic ring.

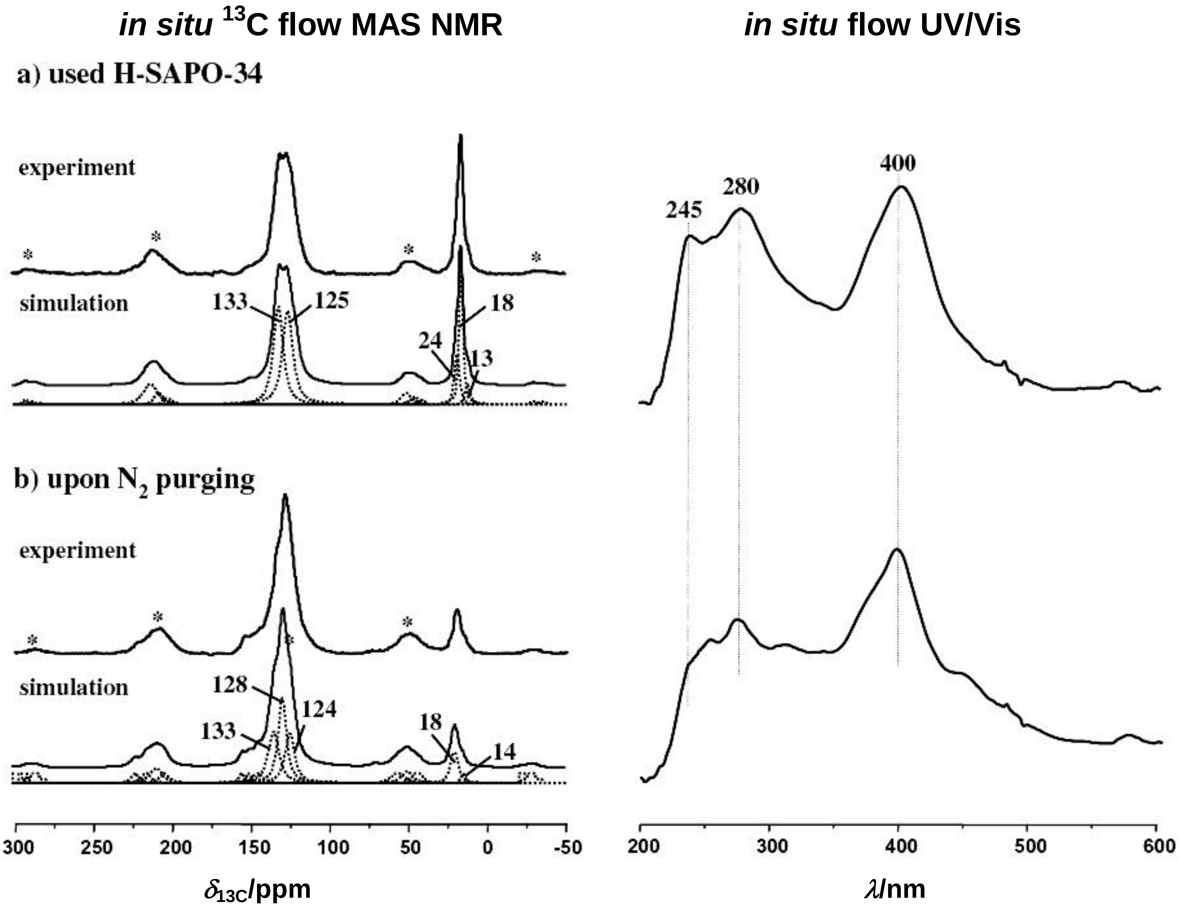
***in situ* ^{13}C flow MAS NMR**

***in situ* flow UV/Vis**

Fig. 2

After increasing the reaction temperature to T = 673 K, a strong decrease of the mean number of alkyl groups to 0.61 mmol/g corresponding to 1.1 alkyl groups per aromatic ring occurred, while the number of aromatic rings per cage was nearly constant (column 4 of **Table 2**). The **decrease of the yield of propene at the reaction temperature of T = 673 K is explained by the lower number of methyl groups per aromatic ring** of the hydrocarbon pool compounds in comparison with the hydrocarbon-pool compounds present at T = 623 K.

In order to study the thermal stability of the organic deposits formed on H-SAPO-34 at T = 673 K, the methanol flow was stopped and the used catalyst was purged with dry nitrogen gas at T = 673 K for 2 h. **Fig. 2b, left**, shows the ^{13}C MAS NMR spectrum of this purged catalyst, recorded at room temperature for quantitative evaluation. The result of the evaluation is summarized in column 5 of **Table 2**. As indicated by these values, the number of ^{13}C atoms in aromatic compounds decreased slightly to 2.45 mmol/g corresponding to *ca.* 0.3 aromatic rings per chabazite cage. Also the number of alkyl groups decreased to 0.34 mmol/g corresponding to 0.8 alkyl groups per aromatic ring. This is a decrease of organic deposits by 25 to 27% in comparison with the used catalyst before purging with dry nitrogen gas at T = 673 K. In the UV/Vis spectra of the purged H-SAPO-34 catalyst, mainly the UV bands of polyalkyl aromatics at λ = 280 nm and a shoulder at λ = 245 nm due to dienes are decreased (compare **Figs. 2a and 2b, right**). This behavior corresponds to the smaller number of polyalkylaromatics observed by ^{13}C MAS NMR spectroscopy. On the other hand, the large band at λ = 400 nm indicates that the polycyclic aromatics occurring on the used H-SAPO-34 catalyst have a high thermal stability and are not affected by purging with nitrogen (**Fig. 2b, right**). Hence, these **polycyclic aromatics are the reason for the catalyst deactivation at high reaction temperatures**.

Catalyst preparation: The silicoaluminophosphate H-SAPO-34 had an $n_{\mathrm{Si}}/(n_{\mathrm{Al}} + n_{\mathrm{Si}} + n_{\mathrm{P}})$ ratio of 0.11 and was synthesized as described elsewhere [20]. Before the use of this zeolite for *in situ* flow experiments, a dehydration was performed with the sample material in a glass tube connected with a vacuum line (see “sample tube system 1” and “vacuum line 1” via link “*In Situ* Solid-State NMR Techniques”). This treatment starts with an evacuation at room temperature for ca. 10 minutes followed by a temperature ramp from room temperature to T = 393 K within 2 hours. At this temperature, the sample is dehydrated for 2 hours. Subsequently, the temperature is increased up to *T* = 723 K within 3 hours and evacuated at this temperature for 12 hours. Finally, the sample tube system is closed via the vacuum valve and disconnected from „vacuum line 1" after this line is ventilated with air. The transfer of the dehydrated sample into the MAS NMR rotor is performed without air contact, e.g., in a glove box purged with dry nitrogen gas (see Section "mini glove box" via link "*In Situ* Solid-State NMR Techniques").

In situ studies: The *in situ* ^{13}C stopped-flow MAS NMR spectra in Figs. 1 and 2 were recorded using the equipment described in Section "equipment 1" and a 7 mm high-temperature MAS NMR probe of Doty Scientific Instruments, modified as described in Section "flow probe 3", both accessible via link "*In Situ* Solid-State NMR Technique".

Via an exhaust tube on top of the MAS NMR rotor, the NMR probe was connected with the sampling loop of a gas chromatograph HP 5890 (Hewlett–Packard) equipped with a Coating Poraplot Q capillary column (Chrompack Plot fused silica, length 50 m, inner diameter 0.32 mm). The exhaust flow containing the volatile reaction products was sampled and analyzed in steps of 15 min. **A constant flow of methane (8 ml/min), added to the methanol feed, was used as an internal GC standard and allowed a quantification of the reaction products**.

High-power proton decoupled (HPDEC) ^{13}C MAS NMR spectra were recorded at the resonance frequency of ν_0 = 100.6 MHz and after excitation with $\pi/2$ pulses. Applying an external intensity standard consisting of dehydrated H-SAPO-34 loaded with $^{13}CH_3OH$, ^{13}C spin-counting was performed with the repetition time of 30 s. All ^{13}C MAS NMR spectra were referenced to tetramethylsilane (TMS).

At the bottom of the 7 mm MAS NMR rotor, a quartz glass window was installed. Via this quartz glass window and using a glass fiber optics, the catalyst inside the rotor was investigated by a fiber-optic UV/Vis spectrometer. Reference UV/Vis spectra of calcined H-SAPO-34 were recorded at the reaction temperature prior to introducing reactants. *In situ* UV/Vis measurements between λ = 200 and 600 nm in the diffuse reflection mode were conducted with an HPSUV1000A Fiber Optic spectrometer, an AvaLight-DH-S deuterium light source, and a glass fiber reflection probe FCR-7UV20-3-SR-S1 by Avantes.

References:

[1] M. Stoeker, *Methanol-to-hydrocarbons: catalytic materials and their behavior*, Microporous Mesoporous Mater. 29 (1999) 3–48, DOI: 10.1016/S1387-1811(98)00319-9.

[2] W. Dai, X. Wang, G. Wu, N. Guan, M. Hunger, L. Li, *Methanol-to-olefin conversion on silicoaluminophosphate catalysts: Effect of Broensted acid sites and framework structures*, ACS Catal. 1 (2011) 292-299, DOI: 10.1021/cs200016u.

[3] U. Olsbye, S. Svelle, M. Bjørgen, P. Beato, T. V. W. Janssens, F. Joensen, S. Bordiga, K. P. Lillerud, *Conversion of Methanol to Hydrocarbons: How Zeolite Cavity and Pore Size Controls Product Selectivity*, Angew. Chem., Int. Ed. 51 (2012) 5810-5831, DOI: 10.1002/anie.201103657.

[4] W. Dai, G. Wu, L. Li, N. Guan, M. Hunger, *Mechanisms of the deactivation of SAPO-34 materials with different crystal sizes applied as MTO catalysts*, ACS Catalysis 3 (2013) 588-596, DOI: 10.1021/cs400007v.

[5] X. Wang, W. Dai, G. Wu, L. Li, N. Guan, M. Hunger, *Verifying the dominant catalytic cycle of the methanol-to-hydrocarbon conversion over SAPO-41*, Catal. Sci. Technol. 4(3) (2014) 688-696, DOI: 10.1039/c3cy00740e.

[6] W. Dai, M. Dyballa, G. Wu, L. Li, N. Guan, M. Hunger, *Intermediates and dominating reaction mechanism during the early stages of the methanol-to-olefin conversion on H-SAPO-41*, J. Phys. Chem. C 119 (2015) 2637-2645, DOI: 10.1021/jp5118757.

[7] W. Dai, C. Wang, M. Dyballa, G. Wu, N. Guan, L. Li, Z. Xie, M. Hunger, *Understanding the early stages of the methanol-to-olefin conversion on H-SAPO-34*, ACS Catal. 5 (2015) 317-326, DOI: 10.1021/cs5015749.

[8] M. Dyballa, P. Becker, D. Trefz, E. Klemm, A. Fischer, H. Jacob, M. Hunger, *Parameters influencing the selectivity to propene in the MTO conversion on 10-ring zeolites: Directly synthesized silicoalumino-type zeolites ZSM-5, ZSM-11, and ZSM-22*, Appl. Catal. A: General 510 (2016) 233-243, DOI: 10.1016/j.apcata.2015.11.017.

[9] M. Dyballa, U. Obenaus, M. Rosenberger, A. Fischer, H. Jakob, E. Klemm, M. Hunger, *Postsynthetic improvement of H-ZSM-22 zeolites for the methanol-to-olefin conversion*, Microporous Meosoporous Mater. 233 (2016) 26-30, DOI: 10.1016/j.micromeso.2016.06.044.

[10] W. Dai, G. Cao, L. Yang, X. Yang, G. Wu, M. Dyballa, M. Hunger, N. Guan, L. Li, *Insights into the catalytic cycle and deactivation of methanol-to olefin conversion over low-silica AlPO-34 zeolites with controlable Broensted acid density*, Catal. Sci. Technol. 7 (2017) 607-618, DOI: 10.1039/c6cy02564a.

[11] L. Yang, T. Yan, C. Wang, W. Dai, G. Wu, M. Hunger, W. Fan, Z. Xie, N. Guan, L. Li, *Role of acetaldehyde in the roadmap from first carbon-carbon bonds to hydrocarbons during the methanol conversion*, ACS Catal. 9 (2019) 6491-6501, DOI: 10.1021/acscatal.9b00641.

[12] M. Seiler, U. Schenk, M. Hunger, *Conversion of methanol to hydrocarbons on zeolite HZSM-5 investigated by in situ MAS NMR spectroscopy under flow conditions and on-line gas chromatography*, Catal. Lett. 62 (1999) 139-145, DOI: 10.1023/A:1019086603511.

[13] W. Wang, M. Seiler, M. Hunger, *Role of surface methoxy species in the conversion of methanol to dimethyl ether on acidic zeolites investigated by in situ stopped-flow (SF) MAS NMR spectroscopy*, J. Phys. Chem. B 105 (2001) 12553-12558, DOI: 10.1021/jp0129784.

[14] M. Hunger, M. Seiler, A. Buchholz, *In situ MAS NMR spectroscopic investigation of the conversion of methanol to olefins on silicoaluminophosphates SAPO-34 and SAPO-18 under continuous flow conditions*, Catal. Lett. 74 (2001) 61-68, DOI: 10.1023/A:1016687014695.

[15] M. Seiler, W. Wang, A. Buchholz, M. Hunger, *Direct evidence for the catalytically active role of the hydrocarbon pool formed on zeolite H-ZSM-5 during the methanol to olefin conversion*, Catal. Lett. 88 (2003) 187-191, DOI: 10.1023/A:1024018023895.

[16] M. Hunger, W. Wang, *Formation of cyclic compounds and carbenium ions by conversion of methanol on weakly dealuminated zeolite H-ZSM-5 investigated via a novel in situ CF MAS NMR/UV-Vis technique*, Chem. Commun. (2004) 584-585, DOI: 10.1039/b315779b.

[17] W. Wang, Y. Jiang, M. Hunger, *Mechanistic investigations of the methanol-to-olefin (MTO) process on acidic zeolite catalysts by in situ solid-state NMR spectroscopy*, Catal. Today 113 (2006) 102-114, DOI: 10.1016/j.cattod.2005.11.015.

[18] Y. Jiang, J. Huang, V.R. Reddy Marthala, Y.S. Ooi, J. Weitkamp, M. Hunger, *In situ MAS NMR-UV/Vis investigation of H-SAPO-34 catalysts partially coked in the methanol-to-olefin conversion under continuous-flow conditions and of their regeneration*, Microporous Mesoporous Mater. 105 (2007) 132-139, DOI: 10.1016/j.micromeso.2007.05.028.

[19] Y. Jiang, J. Huang, J. Weitkamp, M. Hunger*, In situ MAS NMR and UV/VIS spectroscopic studies of hydrocarbon pool compounds and coke deposits formed in the methanol-to-olefin conversion on H-SAPO-34*, Stud. Surf. Sci. Catal. 170 (2007) 1137-1144, DOI: 10.1016/S0167-2991(07)80970-0.

[20] M. Kang, T. Inui, *Dynamic reaction characteristics affected by water molecules during the methanol to olefin conversion on NiAPSO-34 catalysts*, J. Mol. Catal. A: Chem. 140 (1999) 55-63, DOI: 10.1016/S1381-1169(98)00211-8.